Control Engineering Practice 101 (2020) 104498

Contents lists available at ScienceDirect

Control Engineering Practice

journal homepage: www.elsevier.com/locate/conengprac

Modelling and control of an IPMC actuated flexible structure: A lumped port Hamiltonian approach ☆

Andrea Mattioni [a], Yongxin Wu [a,*], Hector Ramirez [c], Yann Le Gorrec [a], Alessandro Macchelli [b]

[a] FEMTO-ST, Univ. Bourgogne Franche-Comté, ENSMM, CNRS, 24 rue Savary, F-25000 Besançon, France
[b] Department of Electrical, Electronic and Information Engineering "Guglielmo Marconi" (DEI), University of Bologna, viale del Risorgimento 2, 40136 Bologna, Italy
[c] Department of Electronic Engineering, Universidad Tecnica Federico Santa Maria, Avenida Espana 1680, Valparaiso, Chile

ARTICLE INFO

Keywords:
EAP actuator
IDA-PBC
Passivity based control
Parameter identification
Anti-damping injection

ABSTRACT

This paper deals with the finite dimensional modelling and control of an electro-active polymer (EAP) actuated flexible structure. This model reproduces the basic mechanical properties of a class of one dimensional flexible endoscope. The flexible structure and the EAP actuator are both modelled as port-Hamiltonian systems. The EAP actuator is interconnected with the flexible structure in a power preserving manner such that the global system is again a PHS. Using the obtained model, two passivity based control strategies are applied to derive the controllers which achieve a desired equilibrium configuration with desired dynamic behaviour. An experimental benchmark composed of the Ionic Polymer Metal Composites patches glued to a flexible beam is used to validate the proposed model and control law.

1. Introduction

The use of medical endoscopes for minimally invasive surgery becomes more and more popular in clinical applications in order to alleviate the suffering of patients. The study of endoscopes can be recalled to the last century (Anderson, Horn, & of Mechanical Engineers, 1967). Due to the recent technological progresses most of medical endoscopes are based on compliant continuum robotics. Continuum robots have been developed for different applications such as: laser manipulators, catheters and micro-endoscopes (Webster I.I.I. & Jones, 2010). Due to the development of smart materials and manufacturing techniques, embedded actuators are used in endoscopic robotics to provide additional degrees of freedom. The authors in Chikhaoui, Rabenorosoa, and Andreff (2014) have proposed a micro endoscope for endonasal skull base surgery. The bending of the endoscope is performed by electro-active polymer (EAP) actuators. One of the most important EAP actuators is the Ionic Polymer Metal Composites (IPMC) which has attractive properties such as: low actuation voltage, ease of fabrication and relatively high strain. These properties have been experimentally pointed out in Shahinpoor and J.K.im (2001). However, the complexity of this material and the flexibility of its structure lead to particularly challenging modelling and control issues.

This paper proposes a 1D physically based model and control strategy for an IPMC actuated flexible structure representative of the mechanical properties of a flexible endoscope suitable for medical applications. To this end, we use the port-Hamiltonian (PH) approach. Port-Hamiltonian systems (PHS) (Maschke & van der Schaft, 1992) have proven to be powerful for the modelling and control of complex physical systems (Duindam, Macchelli, Stramigioli, & Bruyninckx, 2009), such as multi-physical (Doria-Cerezo, Batlle, & Espinosa-Perez, 2010) and non-linear (Ramírez, Le Gorrec, Maschke, & Couenne, 2016). This approach has been generalized to distributed parameter systems described by partial differential equations (Le Gorrec, Zwart, & Maschke, 2005; Ramírez, Le Gorrec, Macchelli, & Zwart, 2014; van der Schaft & Maschke, 2002) and irreversible thermodynamic systems (Ramírez, Maschke, & Sbarbaro, 2013). PHS modelling is based on the characterization of energy exchanges between the different components of a system. This framework is particularly adapted for the modular modelling of multi-physical systems. Hence, it is well suited for the modelling of flexible structure actuated with IPMC patches. A precise PH model of IPMC actuators accounting for multi-scale phenomena has been proposed in Nishida, Takagi, Maschke, and Osada (2011) but we shall consider in this paper a simplified equivalent lumped electrical circuit coping with the main dynamics of the actuator. On

☆ This work has been supported by the French–German ANR-DFG INFIDHEM project (contract: ANR-16-CE92-0028), the EIPHI Graduate School (contract ANR-17-EURE-0002) and the European Commission Marie Skłodowska-Curie Fellowship, ConFlex ITN Network (Reference code: 765579). The second author has received founding from Bourgogne-Franche-comté Region ANER 2018Y-06145. The third author acknowledges Chilean FONDECYT 1191544 and CONICYT BASAL FB0008 projects.

* Corresponding author.
E-mail address: yongxin.wu@femto-st.fr (Y. Wu).

https://doi.org/10.1016/j.conengprac.2020.104498
Received 20 December 2019; Received in revised form 3 April 2020; Accepted 2 June 2020
Available online xxxx
0967-0661/

the other hand, the PHS approach is well suited for the application of passivity based control tools with clear physical interpretation, such as energy shaping and control by interconnection and damping assignment (IDA-PBC) (Macchelli, Le Gorrec, Ramírez, & Zwart, 2017; Ortega & Garcia-Canseco, 2004; Ortega, van der Schaft, Mareels, & Maschke, 2001; Ortega, van der Schaft, Maschke, & Escobar, 2002).

The main contributions of this paper are the proposition of a lumped scalable model suitable for the modelling of flexible actuated structures, different control strategies which take into account the electro-mechanical coupling and the experimental validation of the approach. Firstly, a simple but realistic approximation model of the IPMC actuated medical endoscope (Chikhaoui et al., 2014) using the PHS formalism is proposed. For this purpose, we consider the model composed of IPMC patches glued on a flexible structure. A 1-D lumped model based on interconnected links is considered to model the flexible structure as shown in Fig. 1. We consider that the bending of the flexible structure is due to the torques generated by the IPMC patches when a voltage is applied on the actuators as shown in Fig. 2. Both the 1-D finite dimensional structure and the IPMC actuators are modelled using PHS and interconnected in a power preserving manner. The final model is non-trivial because of the electro-mechanical/mechano-electrical coupling between the flexible structure and the IPMC actuator. Then, two passivity based control strategies, IDA-PBC and the Control by Interconnection-Proportional Integral control are used to achieve a desired equilibrium position of the flexible structure with guaranteed performances. Because of the inter-domain coupling, the closed-loop Lyapunov function has to contain cross terms between electrical and actuated mechanical variables which is also studied in Delgado and Kotyczka (2014). In order to properly select the cross terms while guaranteeing the overall stability, a set of auxiliary design parameters are defined and used to solve the matching conditions associated with the control design problem. Finally an experimental set-up which reproduces the endoscope's behaviour is used to validate the proposed model and to test the effectiveness of the control design method.

The paper is organized as follows: Section 2 presents the PH formulation of the IPMC actuated flexible structure. In Section 3, different passivity based control designs to achieve desired closed loop performances are proposed. The identification of parameters and the model validation on an experimental set-up are presented in Section 4. The simulation and the experimental results are shown in Section 5 to show the effectiveness of the proposed control laws. Some final remarks and perspectives of future works are given in Section 6.

2. PHS Modelling of IPMC actuated flexible structure

The flexible structure is approximated by a mechanical structure composed of n inertia interconnected through flexible joints made up with springs and dampers as shown in Fig. 1. We assume a planar model, and so all the links are allowed to move only in the x-y plane.

We suppose that the flexible structure is under-actuated and that there are $m \leq n$ IPMC actuators inducing torques on $m \leq n$ joints as shown in Fig. 2. Each (actuated or non-actuated) joint of the flexible structure contains a spring and a damper, as shown in Fig. 1.

2.1. PHS Formulation of a flexible structure

In this subsection, we introduce the PH model of the IPMC actuated flexible structure shown in Fig. 1. The parameters of the n-degrees of freedom mechanism ($i = 1, 2, \dots, n$) are:

- q_i the ith joint angular;
- m_i the ith link's mass;
- I_i the moment of inertia about the axe passing through the Centre of Mass (CoM) of the ith link;
- a_i length of the ith link;
- a_{Ci} distance between the ith Joint and the CoM of the ith link;

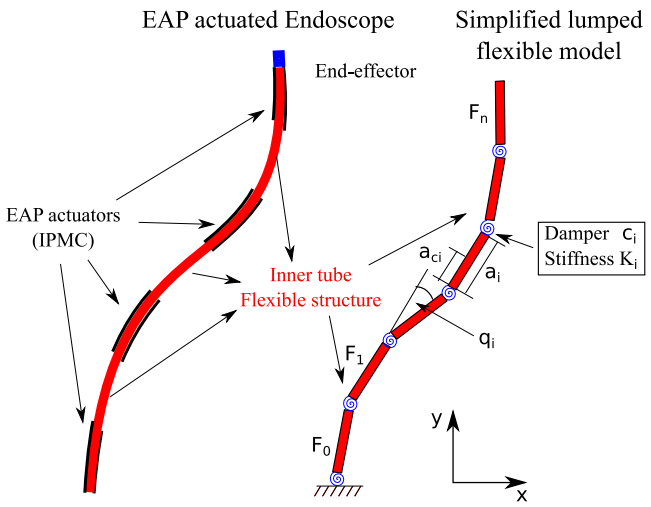

Fig. 1. Lumped parameters flexible structure.

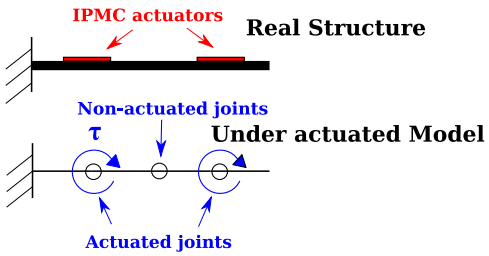

Fig. 2. Flexible structure modelling with the actuators.

- τ_i applied torque on the ith joint;
- $\tilde{K}_i$ stiffness of the ith joint;
- c_i viscous damping at the ith joint;
- P_i E_i Potential and Kinetic energy of the ith link.
- F_0 is the inertial frame;
- F_i is the reference frame attached to the CoM and with axe parallel to the principal axe of inertia of the ith link .

2.1.1. The Hamiltonian function

In this subsection we derive the Hamiltonian function of the flexible structure with respect to the chosen coordinate frame. The Hamiltonian corresponds to the total mechanical energy which is the sum of the kinetic and potential energies. The kinetic energy of the ith link has the form

$$E_i = \frac{1}{2} m_i v_{Ci}^T v_{Ci} + \frac{1}{2} \omega_i^T I_i \omega_i, \tag{1}$$

where v_{Ci} is the velocity of the centre of mass (CoM) of the ith link, ω_i is the angular velocity of the ith link with respect to F_0, I_i is the inertia matrix of the ith link with respect to F_i. The goal is to express the kinetic energy of every link only with respect to the joint angular velocities $\dot{q}_i$ (derivatives of every joint angular). Thanks to the rigidity of the links, it is possible to relate both the velocities of the CoM v_{Ci} and the angular velocities ω_i to the joint angular velocities $\dot{q}_i$. The relation that links joint angular velocities to angular velocities is trivial

$$\omega_i = \dot{q}_1 + \dot{q}_2 + \cdots + \dot{q}_i. \tag{2}$$

This relation can be expressed through the use of the so called angular Jacobian,

$$\omega_i = J_\omega^i \dot{q}, \tag{3}$$

where $q = [q_1, \dots, q_i]^T$ and $\dot{q} = [\dot{q}_1, \dots, \dot{q}_i]^T$. In this case, the angular Jacobian does not depend on the angular displacements. This is not

the case for the Jacobian related to the velocities of the centre of mass. The velocity Jacobian of the ith link is obtained by differentiating the position of the ith centre of mass with respect to time in the F_0 frame,

$$q_{Ci} = \begin{bmatrix} x_{Ci} \\ y_{Ci} \end{bmatrix} = \begin{bmatrix} f_{xi}(q) \\ f_{yi}(q) \end{bmatrix} = f_i(q), \tag{4}$$

where,

$$f_{xi}(q) = \sum_{k=1}^{i-1} a_k \cos\left(\sum_{j=1}^{k} q_j\right) + a_{Ci} \cos\left(\sum_{k=1}^{i} q_k\right),$$
$$f_{yi}(q) = \sum_{k=1}^{i-1} a_k \sin\left(\sum_{j=1}^{k} q_j\right) + a_{Ci} \sin\left(\sum_{k=1}^{i} q_k\right).$$

Differentiating q_{Ci} with respect to time, we obtain $\dot{q}_{Ci} = v_{Ci} = \frac{\partial f_i(q)}{\partial q}\dot{q}$, hence the velocity Jacobian is

$$J_v^i = \frac{\partial f_i(q)}{\partial q}. \tag{5}$$

Now it is possible to express the kinetic energy of every link with respect to the derivative of the displacement vector

$$E_i = \frac{1}{2}\dot{q}^T \left(m_i J_v^{iT}(q) J_v^i(q) + J_\omega^{iT} I_i J_\omega^i\right)\dot{q}. \tag{6}$$

The total kinetic energy of the flexible structure is then

$$E = \frac{1}{2}\dot{q}^T M(q)\dot{q}, \tag{7}$$

where $M(q)$ is the mass matrix of the system, given by

$$M(q) = \sum_{i=1}^{n} \left(m_i J_v^{iT}(q) J_v^i(q) + J_\omega^{iT} I_i J_\omega^i\right). \tag{8}$$

The mass matrix allows to relate the generalized velocity with the momentum of the mechanical system

$$p = M(q)\dot{q}, \tag{9}$$

where $p = \begin{bmatrix} p_1 & p_2 & \cdots & p_n \end{bmatrix}^T$. The kinetic energy expressed as a function of the momentum is then

$$E(q,p) = \frac{1}{2}p^T M^{-1}(q) p. \tag{10}$$

In our framework we are supposing that the work plane is parallel to the ground, therefore we ignore the effect of the gravity on the dynamics of the system. Then, the potential energy is only due to the springs deformation. To find the potential energy we first define the stiffness matrix of the system

$$K = \text{diag}\begin{bmatrix} \tilde{K}_1, & \tilde{K}_2, & \cdots, & \tilde{K}_n \end{bmatrix}. \tag{11}$$

The constitutive relation between elastic torques and springs deformation is given by $\tau_e = Kq$, hence the total potential energy is

$$P(q) = \frac{1}{2}q^T K q. \tag{12}$$

Finally, the Hamiltonian, *i.e.*, the total energy of the flexible structure, is given by

$$H_b(q,p) = E(q,p) + P(q) = \frac{1}{2}p^T M^{-1}(q) p + \frac{1}{2}q^T K q. \tag{13}$$

2.2. The port-Hamiltonian model of the flexible structure

By choosing as state vector of the flexible structure $x_b = [q,p]^T$, we can write the port-Hamiltonian representation (Maschke & van der Schaft, 1992) of the system

$$\begin{cases} \dot{x}_b &= \left(J_b - R_b\right)\frac{\partial H_b(x_b)}{\partial x_b} + g_b u_b \\ y_b &= g_b^T \frac{\partial H_b(x_b)}{\partial x_b} \end{cases} \tag{14}$$

with

$$J_b = \begin{bmatrix} 0 & I_n \\ -I_n & 0 \end{bmatrix}, \quad R_b = \begin{bmatrix} 0 & 0 \\ 0 & C_n \end{bmatrix}, \quad g_b = \begin{bmatrix} 0 \\ g_m \end{bmatrix}$$

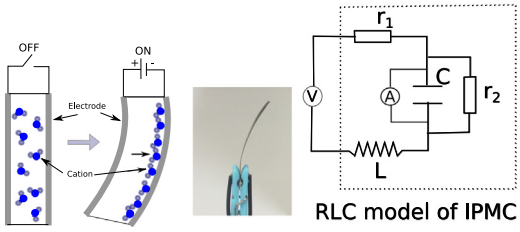

Fig. 3. IPMC bending principle and its electrical model.

with $C_n = \text{diag}\begin{bmatrix} c_1, & c_2, & \cdots, & c_n \end{bmatrix}$, a positive diagonal matrix containing the viscous friction coefficients of the dampers associated with the respective joints. The structural matrix $J_b = -J_b^T$ represents the energy exchanges in the system, while the damping matrix $R_b = R_b^T \geq 0$ captures the internal dissipation of the system. The flexible structure is under-actuated on $m \leq n$ joints, thus the input vector of external torques $u_b = [\tau_1, \tau_2, \ldots \tau_m]^T \in \mathbb{R}^m$ and $g_m \in \mathbb{R}^{n\times m}$. The power conjugate output $y_b \in \mathbb{R}^m$ is the set of angular velocities on the actuated joints. The system is passive. In fact, the Hamiltonian is such that $H_b > 0$ and $H(0) = 0$, moreover its time derivative satisfies:

$$\dot{H}_b = -\frac{\partial H_b}{\partial x_b}^T R_b \frac{\partial H_b}{\partial x_B} + y_b^T u_b \leq y_b^T u_b. \tag{15}$$

2.3. The IPMC actuator model

The bending of the IPMC with respect to the applied voltage is mainly attributed to the cations flux and polar solvents in the polymer membrane diffusion between the electrodes (see left side in Fig. 3) (Shahinpoor & J.K.im, 2001). A multiscale model of an IPMC actuator has been proposed in Nishida et al. (2011). It details the main physical phenomena involved in this multiphysical actuator. In this work, since we assume perfect interconnection between the actuator and the beam, the mechanical contribution of the IPMC actuator is considered as part of the flexible structure. Therefore, we use a simplified and control oriented model for the IPMC'S electric dynamics. This model is based on the lumped RLC equivalent circuit that has been proposed in Gutta, S.L.ee, B.T.rabia, and Yim (2009) and Yim, Trabia, Renno, Lee, and Kim (2006) (right side of Fig. 3). The output torque of the IPMC is proportional to the voltage across the capacitor. The interconnection ports are placed across the capacitor.

The electrical model of the IPMC actuator can be written as

$$\begin{cases} \begin{bmatrix} \dot{\varphi} \\ \dot{Q} \end{bmatrix} = \begin{bmatrix} -r_1 & -1 \\ +1 & -\frac{1}{r_2} \end{bmatrix} \begin{bmatrix} \frac{\partial H_a}{\partial \varphi} \\ \frac{\partial H_a}{\partial Q} \end{bmatrix} + \begin{bmatrix} 1 \\ 0 \end{bmatrix} u(t) + \begin{bmatrix} 0 \\ 1 \end{bmatrix} u_a(t) \\ y = \begin{bmatrix} 1 & 0 \end{bmatrix} \begin{bmatrix} \frac{\partial H_a}{\partial \varphi} \\ \frac{\partial H_a}{\partial Q} \end{bmatrix}, \qquad y_a = \begin{bmatrix} 0 & 1 \end{bmatrix} \begin{bmatrix} \frac{\partial H_a}{\partial \varphi} \\ \frac{\partial H_a}{\partial Q} \end{bmatrix} \end{cases} \tag{16}$$

where the total energy of the system is defined as the sum of the magnetic and electric energies

$$H_a = \frac{1}{2}\frac{Q^2}{C} + \frac{1}{2}\frac{\varphi^2}{L}. \tag{17}$$

and where the state vector is $x_a = [\varphi, Q]^T$ with φ the flux and Q the charge of the capacitor, r_1 and r_2 are the resistances, u is the applied voltage on the IPMC actuator and y is the current in the inductance and y_a is the voltage across the capacitor. Furthermore the torque applied on the flexible structure is generated by y_a with a constant coefficient $[k] = \frac{\text{N·m}}{\text{V}}$, *i.e.*, $u_b = \tau = k y_a$. From the power conserving interconnection, u_a is the current applied on the capacitor due to the mechanical movement of the structure, *i.e.*, $u_a = i_a = -k y_b$. The interconnection relation is defined by

$$\begin{bmatrix} u_b \\ u_a \end{bmatrix} = \begin{bmatrix} 0 & k \\ -k & 0 \end{bmatrix} \begin{bmatrix} y_b \\ y_a \end{bmatrix}. \tag{18}$$

As mentioned before, we consider an under-actuated system, *i.e.*, $m < n$. We shall split the configuration coordinates into actuated and non-actuated ones, *i.e.*, $q = [q_1, q_2]^T$ and $p = [p_1, p_2]^T$ with $q_1, p_1 \in \mathbb{R}^m$ and $q_2, p_2 \in \mathbb{R}^{n-m}$. Thus the interconnected model of the flexible structure and the IPMC actuators can be written as

$$\begin{aligned}\begin{bmatrix}\dot{q}\\ \dot{p}\\ \dot{\varphi}\\ \dot{Q}\end{bmatrix} &= \begin{bmatrix}0 & I_n & 0 & 0\\ -I_n & -C_n & 0 & K_c\\ 0 & 0 & -R_{1m} & -I_m\\ 0 & -K_c^T & I_m & -R_{2m}\end{bmatrix}\begin{bmatrix}\frac{\partial H}{\partial q}\\ \frac{\partial H}{\partial p}\\ \frac{\partial H}{\partial \varphi}\\ \frac{\partial H}{\partial Q}\end{bmatrix} + \begin{bmatrix}0\\ 0\\ I_m\\ 0\end{bmatrix} u\\ y &= \begin{bmatrix}0 & 0 & I_m & 0\end{bmatrix}\begin{bmatrix}\frac{\partial H}{\partial q}\\ \frac{\partial H}{\partial p}\\ \frac{\partial H}{\partial \varphi}\\ \frac{\partial H}{\partial Q}\end{bmatrix},\end{aligned} \tag{19}$$

where $u, y \in \mathbb{R}^m$ and 0 are zero matrices of appropriate dimensions, $R_{1m} = \text{diag}[r_1, r_1, \dots, r_1] \in \mathbb{R}^{m\times m}$, $R_{2m} = \text{diag}[1/r_2, 1/r_2, \dots, 1/r_2] \in \mathbb{R}^{m\times m}$ are the resistance matrices and the coupling matrix K_c is

$$K_c = \begin{bmatrix}K_m\\ 0\end{bmatrix} \in \mathbb{R}^{n\times m} \tag{20}$$

with $K_m = \text{diag}[k_1, k_2, \dots, k_m] \in \mathbb{R}^{m\times m}$.

The total Hamiltonian of the interconnected system is:

$$\begin{aligned}H &= H_a + H_b\\ &= H^Q(x) + H^\varphi(x) + E(x) + P(x)\\ &= \tfrac{1}{2}Q^T C^{-1} Q + \tfrac{1}{2}\varphi^T L^{-1}\varphi + \tfrac{1}{2}p^T M^{-1} p + \tfrac{1}{2}q^T K q.\end{aligned} \tag{21}$$

with the capacitance matrix $C = \text{diag}[C_1, C_2, \dots, C_m]$ and the inductance matrix $L = \text{diag}[L_1, L_2, \dots, L_m]$.

3. Control design

For the current application the control objective is to change the equilibrium position of the IPMC actuated beam and assign a desired performance in terms of settling time and overshoot. Due to the fact that, unlike classical electro-mechanical systems, such as DC-motors, the equivalent electrical circuit has a pervasive dissipative term, at first both charge and magnetic flux equilibria have to be changed. Secondly, from an energy balance perspective the dissipation obstacle (van der Schaft, 2017) does not allow to use control by interconnection techniques for the control synthesis. As a consequence we use interconnection and damping assignment passivity based control (IDA-PBC) (Ortega & Garcia-Canseco, 2004; Ortega et al., 2001, 2002). The main idea is to match the open-loop system with a target system by using state feedback control law.

Proposition 1 (*Ortega et al., 2002*)**.** *Consider the open loop system:*

$$\dot{x} = (J - R)\frac{\partial H}{\partial x} + g(x)u. \tag{22}$$

Define an asymptotically stable PHS target system

$$\dot{x} = \left(J_d - R_d\right)\frac{\partial H_d}{\partial x} \tag{23}$$

with matrices $J_d(x) = -J_d(x)^T$, $R_d(x) = R_d^T(x) \geq 0$ and function H_d that verifies the PDE:

$$g^\perp\left(J_d - R_d\right)\frac{\partial H_d}{\partial x} = g^\perp (J - R)\frac{\partial H}{\partial x}, \tag{24}$$

with $g^\perp$ a full rank left annihilator of g, i.e., $g^\perp g = 0$ and the Hamiltonian function $H_d(x)$ such that

$$x^* = arg\min H_d(x). \tag{25}$$

with x^* the equilibrium to be stabilized. The closed-loop system (22) with the feedback law $u = \beta(x)$, where

$$\beta(x) = \left(g^T g\right)^{-1} g^T\left(\left(J_d - R_d\right)\frac{\partial H_d}{\partial x} - (J - R)\frac{\partial H}{\partial x}\right) \tag{26}$$

behaves as the target system (23) with x^* (asymptotically) stable.

Remark 2 (*Anti Damping Injection*)**.** The choice of the new damping matrix R_d affects the rise time of the closed loop system response. To speed up the system it is possible to choose $0 \leq R_d \leq R$. This scenario corresponds to an anti-damping injection: the parameter of the resulting damping injection is negative.

In our application we perform energy shaping on the position, charge and magnetic flux, which are coupled through a dissipative electrical circuit. This implies that the closed-loop energy/Lyapunov function will present cross terms between these variables. Hence in the following Proposition we present a non-trivial solution to the control problem. For the sake of readability of the paper, the Proof of this Proposition is given in Appendix.

Proposition 3. *Consider the open loop system (19) and define an asymptotically stable PHS target system:*

$$\dot{x} = \left(J_d - R_d\right)\frac{\partial H_d}{\partial x} \tag{27}$$

with the desired structure matrix $J_d = J$ and the desired damping matrix defined as

$$R_d = R + R_c \quad with \quad R_c = diag\begin{bmatrix}0, & 0, & r_c, & 0\end{bmatrix}. \tag{28}$$

with $r_c > -R_{1m}$. The desired closed-loop Hamiltonian is defined as

$$H_d(x) = \frac{1}{2}x_d^T Q_d x_d \tag{29}$$

where $x_d = \left[\left(q_1 - q_1^*\right), \quad q_2, \quad p, \quad (\varphi - \varphi^*), \quad (Q - Q^*)\right]^T$ and the symmetric matrix Q_d is defined as:

$$Q_d = \begin{bmatrix}K_1' & 0 & 0 & K_m R_{2m}\tilde{C} & K_m\tilde{C}\\ * & K_2 & 0 & 0 & 0\\ * & * & M^1 & 0 & 0\\ * & * & * & L'^{-1} & R_{2m}\tilde{C}\\ * & * & * & * & C'^{-1}\end{bmatrix} \tag{30}$$

with $\tilde{C} = \left(C'^{-1} - C^{-1}\right)$, $K_1' = K_1 + K_m^2\tilde{C}$ and $L'^{-1} = L^{-1} + R_{2m}^2\tilde{C}$. The desired equilibrium position of the system is $x^* = \left[q_1^*, 0, 0, \varphi^*, Q^*\right]$ with

$$Q^* = \frac{K_1 C}{K_m}q_1^*, \qquad \varphi^* = \frac{R_{2m} L K_1}{K_m}q_1^*, \tag{31}$$

and $x^* = arg\min H_d(x)$. Then the system (19) with feedback law $u = \beta(x)$, where

$$\begin{aligned}\beta(x) = \quad & -\left(R_{1m}L'^{-1} + R_{2m}\tilde{C}\right)(\varphi - \varphi^*)\\ & -\left(R_{1m}R_{2m} + I_m\right)K_m\tilde{C}\left(q_1 - q_1^*\right)\\ & -\left(R_{1m}R_{2m}\tilde{C} + C'^{-1}\right)(Q - Q^*)\\ & + R_{1m}L^{-1}\varphi + C^{-1}Q - r_c L'^{-1}\varphi\end{aligned} \tag{32}$$

behaves as the target system (27) with x^* (asymptotically) stable.

Proof. See Appendix. □

The control law (32) that corresponds to the general solution of the control problem stated in Proposition 3 is a state feedback. As a consequence its implementation requires the use of an observer. A possible solution consists in choosing the control parameters such that (32) can be implemented as an output feedback. Indeed since the output of the PHS model is the electrical current of the actuator *i.e.*, $i = L'^{-1}\varphi$, an appropriate choice of the control parameters leads to an output feedback rather than a state feedback, simplifying its experimental implementation while guaranteeing the global stability.

Proposition 4. *Consider the control law (32) and assume R_{2m} negligible since the resistance in parallel to the capacitor r_2 is large enough. Then (32) becomes a Proportional integral control:*

$$u = -\tilde{C}\int_0^t i(s)ds + \left(K_m\tilde{C} + \frac{K_1 C}{K_m C'}\right)q_1^* - r_c i. \tag{33}$$

where $i \in \mathbb{R}^m$ is the measured current.

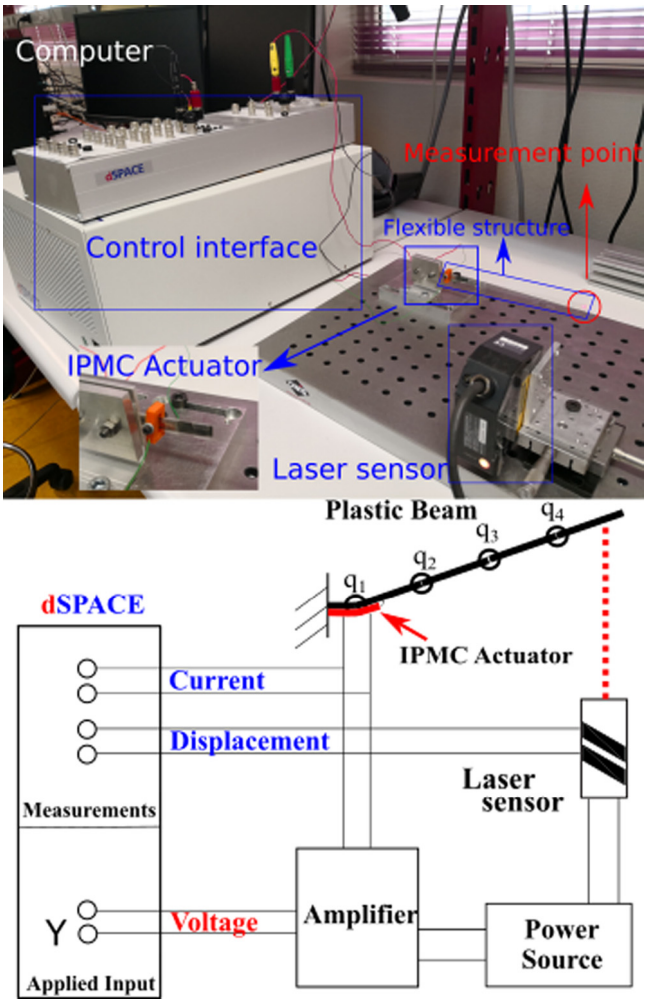

Fig. 4. Experimental set-up.

Proof. We assume the dissipation matrix R_{2m} is negligible then the control law (32) becomes:

$$\begin{aligned} u_c &= -R_{1m}L'^{-1}(\varphi-\varphi^*) - K_m\tilde{C}\left(q_1-q_1^*\right) \\ &\quad -C'^{-1}(Q-Q^*) + R_{1m}L^{-1}\varphi + C^{-1}Q \\ &= -R_{1m}\left(L'^{-1}-L^{-1}\right)\varphi - K_m\tilde{C}q_1 - \tilde{C}Q \\ &\quad + K_m\tilde{C}q_1^* + C'^{-1}Q^* \end{aligned} \tag{34}$$

Because $L'^{-1} = L^{-1} + R_{2m}^2\tilde{C}$, then $L'^{-1} = L^{-1}$ with $R_{2m} \approx 0$. The above control law becomes

$$\begin{aligned} u_c &= -K_m\tilde{C}q_1 - \tilde{C}Q + K_m\tilde{C}q_1^* + C'^{-1}Q^* \\ &= -\tilde{C}\left(K_mq_1 + Q\right) + K_m\tilde{C}q_1^* + C'^{-1}Q^* \end{aligned} \tag{35}$$

where q_1, Q and $\varphi \in \mathbb{R}^m$, and is completed by damping injection through

$$u = u_c - r_c\frac{\varphi}{L'} = u^* - r_ci. \tag{36}$$

By taking into account the last equation of the complete system (19) and $R_{2m} = 0$, one can get:

$$i = y = k_1\dot{q}_1 + \dot{Q} \tag{37}$$

and since $Q^* = \frac{K_1C}{K_m}q_1^*$, the control law (35) becomes:

$$u_c = -\tilde{C}\int_0^t i(s)ds + + \left(K_m\tilde{C} + \frac{K_1C}{K_mC'}\right)q_1^* \tag{38}$$

Substituting the former equation in (36), we obtain Eq. (33). □

Table 1
Physical parameters of the flexible beam.

L	Length	0.16 m
W	Width	7×10^{-3} m
T	Thickness	0.22×10^{-3} m
ρ	mass density	936 kg/m^3

Table 2
Fixed parameters of the Lumped parameter model.

a_i	Length of the $i-$link	4×10^{-3} m
m_i	Mass of the $i-$link	0.58×10^{-4} kg
I_i	Inertia of CoM of the $i-$link	0.77×10^{-8} kg m^3

Other passivity based control strategies can be used to overcome the dissipation obstacle, using an output feedback instead of a state feedback. For instance the Control by Interconnection-Proportional Integral (CbI-PI) method based on a power-shaping output (Borja, Cisneros, & Ortega, 2016) uses a "power shaping output" y_{ps} instead of the classical conjugated output y (19):

$$y_{ps} = -g^TF^{-T}\left(F\frac{\partial H}{\partial x} + gu\right), \tag{39}$$

where $F = J - R$ is defined in (19) and H is the open loop energy defined in (21). Following Borja et al. (2016), we implement the control law as:

$$u_{PS} := \begin{bmatrix} I + K_Pg^TF^{-T}g \end{bmatrix}^{-1}\begin{bmatrix} -K_I(\gamma(x)+\kappa) \\ +K_Pg^TF^{-T}F\nabla H(x) \end{bmatrix} \tag{40}$$

where $\gamma(x)$ is a function defined by the relation $\dot{\gamma}(x) = y_{ps}$, $K_I, K_P > 0$ are the control design parameters and $\kappa = K_I^{-1}g^{*\dagger}F^*(\nabla H(x))^* - \gamma^*$[1] is computed from the desired equilibrium point x^*.

For the present "power shaping output" y_{ps} corresponds to the currents flowing in the resistances R_{2m}, and since it is a fictitious current inside the IPMC, it is not directly accessible. As for the control derived in Proposition 3, a state observer is need to implement the controller.

4. Identification and experimental validation

For the identification and experimental validation we consider a polyethylene flexible structure equipped with one IPMC actuator. The complete experimental set-up is shown in Fig. 4.

A dSPACE board and a computer (with Matlab Simulink) is used to generate the control signals $U \in [0, 7\text{V}]$ on the IPMC, to get the measurements and to implement the controller. The measurements are the displacement of the flexible structure and the applied voltage to the IPMC actuator. The displacement is measured by a laser displacement sensor from KEYENCE company (LK-G152).

4.1. Identification of the flexible-structure parameters

In this section, we identify the parameters used for the finite dimensional modelling of the flexible structure. The physical parameters related to the considered polyethylene beam are summarized in Table 1. It is considered that the flexible structure is composed of four links ($n = 4$) and actuated at the first joint with an IPMC actuator ($m = 1$). The known parameters of the PHS lumped parameter model (14) are shown in Table 2.

The unknown parameters are the stiffness and the damping coefficients of every joint. We shall assume a uniform beam, hence we assume identical stiffness K_i and damping C_i coefficients. In order to identify these parameters, we measure the displacement at the end of the beam with the laser sensor. The positioning of the laser sensor is at 5 mm from the tip of the flexible structure in equilibrium position.

[1] $g^\dagger$ stands for the pseudo-inverse of the vector g.

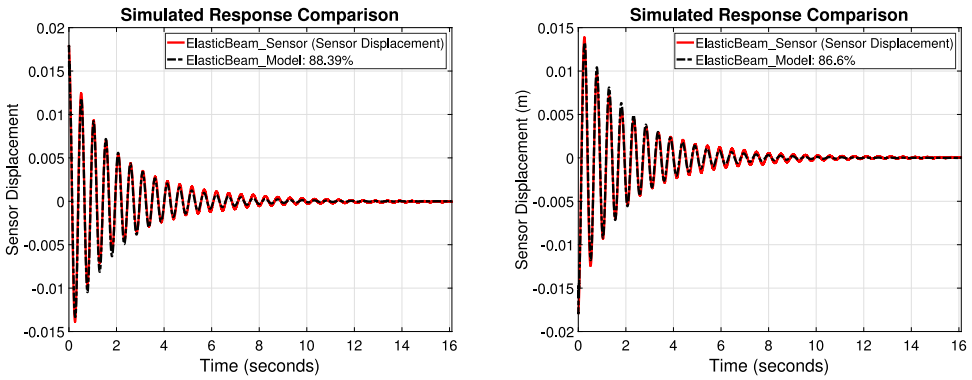

Fig. 5. (lhs) Parameter estimation with linear stiffness for every joints. The displacement measurement is taken at $x_s = 15.5$ cm. (rhs) Model validation with $x_s = 14$ cm.

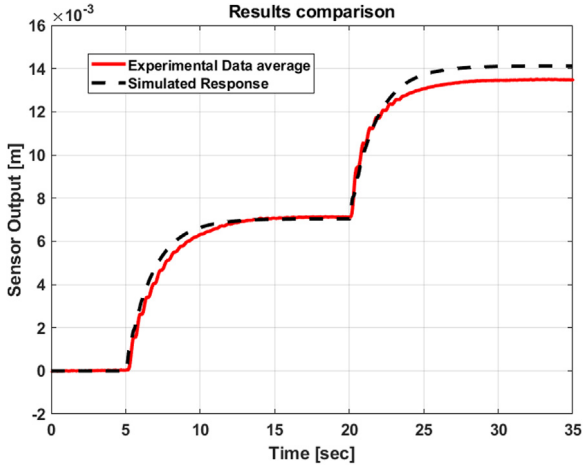

Fig. 6. IPMC actuation identification for $U_1 = 2$ V and $U_2 = 4$ V.

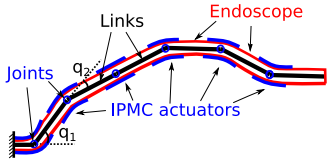

Fig. 7. 6 links structure representation of the endoscope.

Table 3
Identified stiffness and damping coefficients.

K_i	Stiffness of the i–joint	10.4×10^{-4} N/m
c_i	Damping of the i–joint	7.682×10^{-6} Pa s

In the current experimental set-up, $n = 4$ and the a_i are given in Table 2. The experimental data used to identify the parameters is the displacement, taken at $x_s = 15.5$ cm.

The identification procedure is performed using Sequential Quadratic Programming (SQP) and trust-region-reflective algorithms (*'fmincon'*). These optimal algorithms for non-linear model identification (*'nlgreyest'*) are implemented in the Matlab Identification Toolbox®.

The identification result is shown in Fig. 5 (lhs). The curve fitting of the model simulation with optimally identified parameters (black dashed line) and the experimental data (red solid line) is satisfying, with a fitting percentage of 88.39%. The identified stiffness and damping coefficients are shown in Table 3.

To validate the identified model, we measure the displacement at a different point, $x_s = 14$ cm with the different initial position, and compare the measurements with the simulation. The results are shown in Fig. 5 (rhs). The fitting percentage is 86.6%.

Table 4
Parameters of the IPMC actuator.

C	5.8×10^{-2} F
r_1	29.75 Ω
r_2	700 Ω

4.2. Identification of the IPMC parameters

The physical parameters of the RLC model of the IPMC are given in Table 4 (Gutta et al., 2009; Nishida et al., 2011; Yim et al., 2006).

The movement of the flexible structure is due to the bending of the IPMC when applying a voltage. Two voltages step inputs are applied, first $U_1 = 2$ V at 5 s, and then $U_2 = 4$ V at 20 s. The measure is the displacement at $x_s = 15.5$ cm. An average of several experimental tests is has been performed in order to avoid environmental perturbations as much as possible. The experimental response is shown in Fig. 6. One can observe that the flexible structure displaces 6.5 mm and 13.8 mm when applying 2 V and 4 V respectively.

Using the same identification procedure as in the previous subsection, the coupling parameter is identified as

$$k = 0.98 \times 10^{-5} \text{N m/V} \tag{41}$$

The simulation result is given in Fig. 6 in red solid line and the experimental data in black dashed line.

Remark 5. In the proposed model, the dynamics of the IPMC actuator are simplified to a RLC circuit and the coupling between the actuator and the flexible structure is also simplified to a constant coefficient k. However, the IPMC actuator has a nonlinear electro-stress diffusion dynamic which is not addressed in this paper. This is why in Fig. 6, the simulation curve (black dashed line) is slightly different from the experimental data (red solid line) at second 22 s.

5. Control implementation by simulation and experimental validation

5.1. Control implementation by simulation

In the following, we consider the case with $n = 6$ and model parameters equal to the ones estimated in the last section. We use the same model for the two control designs (IDA-PBC and CbI-PI) and for the simulations.

The desired configuration of the endoscope (Fig. 7) is defined by the angular position $q^* = \begin{bmatrix} q_1^* & -\frac{q_1^*}{2} & 0 & -\frac{q_1^*}{2} & -\frac{q_1^*}{2} & \frac{q_1^*}{2} \end{bmatrix}$ where $q_1^* = 0.085$ rad. We compute the control law (40) with the equilibrium

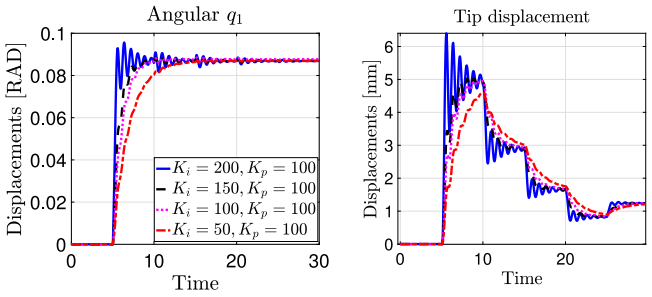

Fig. 8. CbI-PI control: (lhs) Angular displacement q_1; (rhs) Tip displacement y_s.

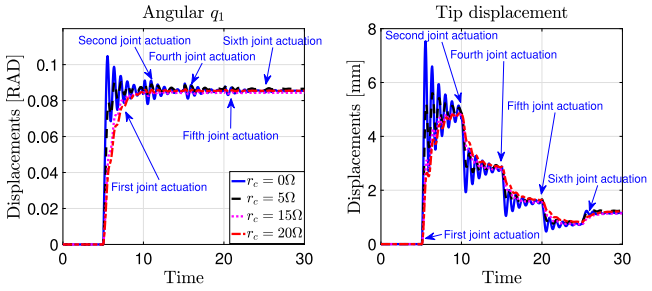

Fig. 9. Proposed IDA-PBC control: (lhs) Angular displacement q_1; (rhs) Tip displacement y_s.

$x^* = \begin{bmatrix} q^* & 0 & Q^* & \varphi^* \end{bmatrix}$, where Q^* and φ^* are computed by (31), with design parameter $C' = 0.005$ F. The different patches are actuated sequentially from the clamped side to the free hand side, *i.e.* the different IPMC patches are actuated at time 5, 10, 15, 20 and 25 seconds, respectively. Fig. 8 shows the angular displacement q_1 (lhs) and the tip displacement y_s (rhs) for different values of K_I and K_P.

Fig. 9 shows the implementation of the control law (33) under same conditions as before for different damping injections terms r_c, while the desired closed loop capacitance is selected such that $C' = 0.005$ F. The responses obtained with the CbI-PI (40) and the IDA-PBC (32) of respectively Figs. 8 and 9 gives very similar results. Hence, because of its simplicity, the output feedback (33) will be implemented on the experimental set-up. In the following two different experimental scenarios are considered. First the structure actuated with one IPMC patch, and then the structure actuated with two patches.

5.2. Flexible structure with one IPMC patch

In this subsection the control strategy of Section 3 is applied and experimentally validated on the flexible structure controlled by using one IPMC actuator. The control law (33) is cast in the single patch actuation case, and implemented using the voltage as control input to the IPMC. Instead of plotting the angular displacement of the joints, the displacement y_s is plotted since it is the quantity that is experimentally measured by the laser sensor, as explained in the previous section. The reference position is given in terms of y_s. The desired angular position q^* can be computed as

$$q^* = \tan^{-1}\left(\frac{y_s}{x_s - \frac{L}{n+1}}\right) \tag{42}$$

where in this case, $y_s^* = 5$ mm, $x_s = 15.5$ cm, $L = 16$ cm and $n = 4$.

The experimental results are shown in Fig. 10. It is shown that without any damping term the raising time can be drastically reduced up to 1 second. However, in this case, since the response of the controlled system is faster, the high frequency modes of the flexible structure are excited and have a significant oscillatory contribution to the time response (black dashed-dotted line with $r_c = 0\Omega$). The use of damping

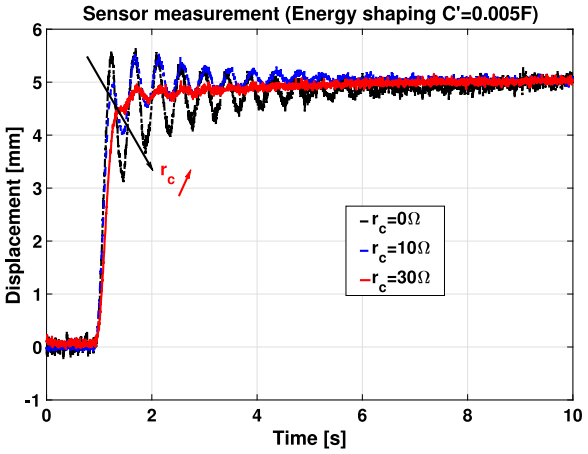

Fig. 10. Controlled response with energy shaping $C' = 0.005$ F. Response time ↗ and oscillation ↘ when r_c ↗.

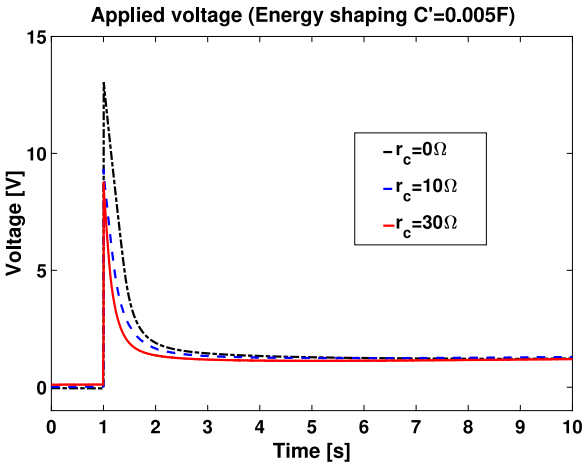

Fig. 11. Applied voltage with energy shaping $C' = 0.01$ F.

injection allows to damps this oscillation. In Fig. 10 one can see that by using the damping term $r_c = 10\Omega$ the step response is less oscillatory (blue dashed line). Finally, a good compromise between oscillations and time response (around 1 second) can be found by choosing $r_c = 30\Omega$ (red solid line).

In Fig. 11, the applied voltage to the IPMC actuator when using control by energy shaping is shown. The controller sends a peak voltage to the IPMC and then decreases until converging to the steady state position.

5.3. Flexible structure with two IPMC patches

In this subsection, we investigate the actuation through two IPMC patches. One patch is placed at the clamped side of the beam as in the previous subsection and the second actuator is placed at the middle of the flexible structure as shown in Fig. 12.

The control objective of the multi-actuated flexible structure is to reach a desired shape for the structure (as shown at the bottom of Fig. 12) with guaranteed performances in terms of settling time and overshoot. In this case, we propose to use the four links structure to design the controller as it provides a good compromise between accuracy and complexity. The actuation is applied to the first and the third joint of the structure respectively. Two KEYENCE laser sensors are used to measure the tip displacement and the middle displacement of the flexible structure.

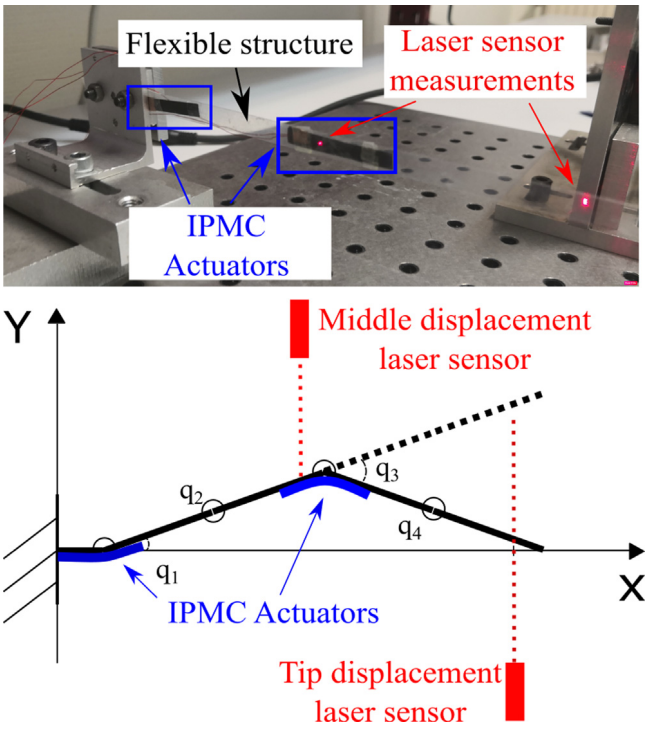

Fig. 12. Multi-actuation experimental set-up.

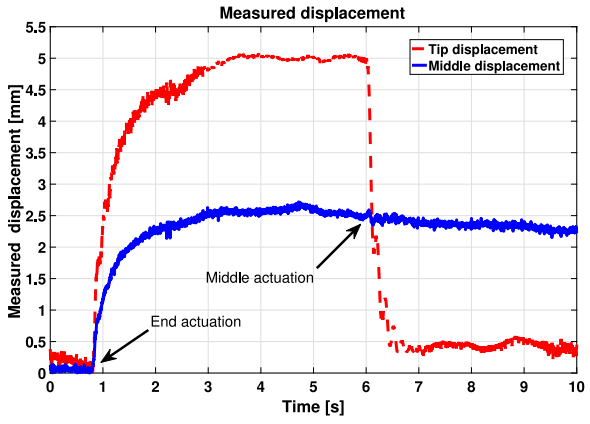

Fig. 13. Tip and middle displacements.

We first move the free end of the structure to the desired position $y_s^* = 5$ mm as in the previous subsection. Then, the desired angular position q_1^* is computed from (42) using $y_s^* = 5$ mm. In a second instance, we bring the free end of the structure to the original position *i.e*, $y_s = 0$ by the second IPMC actuator placed at the middle of the structure (third joint). It applies the angular position $q_3^* = -2q_1^*$. Hence the desired angular positions corresponding to the desired shape of the structure are $q^* = \begin{bmatrix} q_1^* & 0 & -2q_1^* & 0 \end{bmatrix}^T$. The control design parameters are $C' = 0.05$ F and $r_c = 30\Omega$ for both actuators.

In Fig. 13, the tip and middle displacement measurements are shown. The red dashed curve is the tip displacement and the blue solid curve is the measurement from the middle laser sensor. First the control law (33) is used to drive the clamped side IPMC actuator such that the tip of the structure moves to the desired position 5 mm and then at 6 s, we control the second IPMC actuator placed at the middle of the structure to drive the tip to its original place. One can observe that the tip displacement (red dashed curve) first goes to the desired position and then goes back to 0 at 6 s. The middle of the flexible structure (blue solid line) first goes to 2.5 mm and does not move anymore apart from a small oscillation at 6 s when the second IPMC is actuated.

6. Final remarks and perspectives

The paper presents a lumped model and control strategy for a class of 1-D IPMC actuated flexible structure using the PHS framework. The model reproduces the main behaviour of the IPMC actuated endoscope and has as main feature that it is easy scalable. The control strategy is based on IDA-PBC, and takes into account the electro-mechanical coupling in the design of the closed-loop Hamiltonian function. The cross terms result in non-trivial matching conditions which are solved by using a set of auxiliary control design parameters. The resulting controller allows to modify the closed-loop equilibrium and shape the closed-loop Hamiltonian.

An experimental set-up has been used to test and validate the proposed model and control strategy. The experimental set-up reproduces the main properties of a compliant bio-medical endoscope process. The comparison between simulations and the experimental data shows that the model reproduces the experimental response in a satisfactory way. Two control strategies are implemented, one which only changes the closed-loop equilibrium and a second one which also shapes the closed-loop energy function. Both controllers asymptotically stabilize the system. It has been shown by means of simulations and experimental tests that by modifying the closed-loop Hamiltonian function the closed-loop response can be effectively tuned and rendered faster. Furthermore, the flexible structure is actuated by two IPMC patches which allow to get a desired configuration of the structure.

There are still several interesting points worth investigating in the future. The actuation of IPMC is very sensible to humidity. During experimentation it has been observed that a humid actuator is more efficient and active than a dryer one. This is due to the physical nature since the bending of the actuator depends on the water molecules in the polymer of the IPMC. Ongoing work is to deal with the parameter uncertainty caused by the humidity and to investigate robust control design. With the same idea, the effect of external perturbations has to be investigated. To this end, a simplified model of the IPMC actuator has been considered, hence the dynamic of the polymer gel diffusion has not been taken into account. Future work will consider a complete IPMC actuator model.

Declaration of competing interest

The authors declare that they have no known competing financial interests or personal relationships that could have appeared to influence the work reported in this paper.

Appendix. Proof of Proposition 3

Proof. In order to get the control law shown in (32), we first define a full rank annihilator $g^\perp$ is

$$g^\perp = \begin{bmatrix} I_m & 0 & 0 & 0 & 0 & 0 \\ 0 & I_{n-m} & 0 & 0 & 0 & 0 \\ 0 & 0 & I_m & 0 & 0 & 0 \\ 0 & 0 & 0 & I_{n-m} & 0 & 0 \\ 0 & 0 & 0 & 0 & 0 & I_m \end{bmatrix}. \tag{A.1}$$

We will not modify the closed-loop interconnection matrix *i.e.*, $J_d = J$. By observing the open-loop system (19) and the fact that the fifth column of the annihilator $g^\perp$ defined in (A.1) is zero, one find that the matching conditions do not depend on the φ coordinates. The desired damping matrix can then be defined as

$$R_d = R + R_c \quad \text{with} \quad R_c = \text{diag}\begin{bmatrix} 0, & 0, & r_c, & 0 \end{bmatrix}. \tag{A.2}$$

This choice of damping matrix leads to the damping injection effect in the closed-loop system without changing any matching condition. We

can use a negative damping injection to increase the response time *i.e.* $r_c < 0$. However, in order to guarantee the stability in the closed-loop system, this negative damping injection has a lower bound $r_c > -R_{1m}$.

By setting $H_d(x) = H(x) + H_c(x)$ the matching condition (24) leads to the following matching equations

$$\frac{\partial H_c}{\partial p} = \frac{\partial H_c}{\partial q_2} = 0, \tag{A.3}$$

$$-\frac{\partial H_c}{\partial q_1} + K_m \frac{\partial H_c}{\partial Q} = 0, \tag{A.4}$$

$$\frac{\partial H_c}{\partial \varphi} - R_{2m} \frac{\partial H_c}{\partial Q} = 0, \tag{A.5}$$

where $q_1 \in \mathbb{R}^m$, $q_2 \in \mathbb{R}^{n-m}$, $p \in \mathbb{R}^n$, $Q, \varphi \in \mathbb{R}^m$, $K_m = \text{diag}[k_1, k_2, \dots, k_m] \in \mathbb{R}^{m\times m}$ and $R_{2m} = \text{diag}[1/r_2, 1/r_2, \dots, 1/r_2] \in \mathbb{R}^{m\times m}$.

We define the desired Hamiltonian as the composition of the desired mechanical potential energy, the desired mechanical kinetic energy and the desired electrical energy

$$H_d(x) = E_d(x) + P_d(x) + H_d^{\varphi}(x) + H_d^{Q}(x). \tag{A.6}$$

From the matching condition (A.3), we find that H_c cannot depend on the momentum variables p. Hence, we define the closed-loop kinetic energy as $E_d(x) = E(x)$. Hence, the only part of the energy that can be modified is $P_d(x)$, $H_d^Q(x)$ and $H_d^{\varphi}(x)$, and more precisely the part that depends on Q, φ and q_1. From the matching conditions (A.4) and (A.5), the desired energy has cross terms between q_1, Q and φ. Hence, we propose the following solution

$$\begin{aligned}
\frac{\partial H_d}{\partial q_1} &= K_1' \left(q_1 - q_1^*\right) + \kappa_1 \left(Q - Q^*\right) + \kappa_3 \left(\varphi - \varphi^*\right) \\
\frac{\partial H_d}{\partial Q} &= C'^{-1} \left(Q - Q^*\right) + \kappa_1 \left(q_1 - q_1^*\right) + \kappa_2 \left(\varphi - \varphi^*\right) \\
\frac{\partial H_d}{\partial \varphi} &= L'^{-1} \left(\varphi - \varphi^*\right) + \kappa_2 \left(Q - Q^*\right) + \kappa_3 \left(q_1 - q_1^*\right)
\end{aligned} \tag{A.7}$$

with K_1', C' and L' the desired stiffness, capacitance and inductance of the closed-system. The constants q_1^*, Q^* and φ^* are the equilibrium position of the closed loop system and κ_i, $i = \{1, 2, 3\}$ are constant cross terms. Now we shall compute the above design parameters such that the desired Hamiltonian satisfies the matching condition (A.4) and (A.5).

Taking (A.7) and the gradient of the open-loop Hamiltonian $\frac{\partial H}{\partial q_1} = K_1 q_1$, $\frac{\partial H}{\partial Q} = C^{-1} Q$ and $\frac{\partial H}{\partial \varphi} = L^{-1}\varphi$ into account, we have that

$$\begin{aligned}
\frac{\partial H_c}{\partial q_1} &= (K_1' - K_1) q_1 - K_1' q_1^* + \kappa_1 \left(Q - Q^*\right) + \kappa_3 \left(\varphi - \varphi^*\right) \\
\frac{\partial H_c}{\partial Q} &= (C'^{-1} - C^{-1}) Q - C'^{-1} Q^* + \kappa_1 \left(q_1 - q_1^*\right) + \kappa_2 \left(\varphi - \varphi^*\right) \\
\frac{\partial H_c}{\partial \varphi} &= (L'^{-1} - L^{-1}) \varphi - L'^{-1} \varphi^* + \kappa_2 \left(Q - Q^*\right) + \kappa_3 \left(q_1 - q_1^*\right)
\end{aligned} \tag{A.8}$$

To find a solution for H_c satisfying (A.8), we select

$$K_1' = K_1 + K_m^2 \tilde{C} \tag{A.9}$$

$$L'^{-1} = L^{-1} + R_{2m}^2 \tilde{C} \tag{A.10}$$

$$\kappa_1 = K_m \tilde{C} \tag{A.11}$$

$$\kappa_2 = R_{2m} \tilde{C} \tag{A.12}$$

$$\kappa_3 = K_m R_{2m} \tilde{C} \tag{A.13}$$

where the matrix $\tilde{C} = \left(C'^{-1} - C^{-1}\right)$ With the above choice, the matching conditions (A.4) and (A.5) are satisfied.

Now we compute the constants K_1', C' and L' such that the closed-loop system is asymptotically stable at the desired equilibrium $\left[q_1^{*T}, Q^{*T}, \varphi^{*T}\right]^T$. From (25) it should be verified that

$$\frac{\partial H_d}{\partial x}(x^*) = 0, \quad \frac{\partial^2 H_d}{\partial x^2}(x^*) > 0. \tag{A.14}$$

From the first equation of (A.14), $q_1 = q_1^*$, $Q = Q^*$ and $\varphi = \varphi^*$ satisfy the following relations

$$\begin{aligned}
K_1' \left(q_1 - q_1^*\right) + K_m \tilde{C} \left(Q - Q^*\right) + K_m R_{2m} \tilde{C} \left(\varphi - \varphi^*\right) = 0 \\
C'^{-1} \left(Q - Q^*\right) + K_m \tilde{C} \left(q_1 - q_1^*\right) + R_{2m} \tilde{C} \left(\varphi - \varphi^*\right) = 0 \\
L'^{-1} \left(\varphi - \varphi^*\right) + R_{2m} \tilde{C} \left(Q - Q^*\right) + K_m R_{2m} \tilde{C} \left(q_1 - q_1^*\right) = 0
\end{aligned} \tag{A.15}$$

From the open-loop dynamic (19), by computing $\dot{x}(x^*, u^*) = 0$, we find that the equilibrium q_1^*, Q^* and φ^* are related as follows

$$Q^* = \frac{K_1 C}{K_m} q_1^*, \qquad \varphi^* = \frac{R_{2m} L K_1}{K_m} q_1^*. \tag{A.16}$$

Finally, to guarantee the equilibrium x^* be the strict minimum of the closed-loop Hamiltonian, the Hessian of H_d should be positive definite at the desired equilibrium. Thus the right inequality of (A.14) yields the following condition on the control design parameter C':

$$\begin{aligned}
&C'^{-1} \geq C^{-1} - \frac{K_1}{K_m^2}, \quad C'^{-1} \geq \frac{K_m^2 C^{-2}}{K_1 + K_m C^{-1}}, \\
&C'^{-1} \geq \frac{\left(K_m^2 L^{-1} + R_m^2 K_1\right) C^{-2}}{K_1 L^{-1} + K_m^2 L^{-1} C^{-1} + R_m^2 K_1 C^{-1}}.
\end{aligned} \tag{A.17}$$

From (A.9) and (A.10) we see that K_1', L' and C' are related. Hence once we choose the parameter C' satisfying the conditions (A.17), the two other parameters are fixed. The proof of the asymptotic stability is straightforward once it is noticed that the desired closed-loop dissipation matrix is equal to the open-loop dissipation matrix, and in particular that the dissipation sub-matrix of the electrical part is full rank. Hence, the asymptotic stability follows in an analog manner as the asymptotic stability of a mass–spring–damper systems (van der Schaft, 2017) by using LaSalle's invariance principle.

Finally from Proposition 1 and the damping injection (A.2), the following control law is obtained:

$$\begin{aligned}
\beta(x) = \; &- \left(R_{1m} L'^{-1} + R_{2m} \tilde{C}\right) \left(\varphi - \varphi^*\right) \\
&- \left(R_{1m} R_{2m} + I_m\right) K_m \tilde{C} \left(q_1 - q_1^*\right) \\
&- \left(R_{1m} R_{2m} \tilde{C} + C'^{-1}\right) \left(Q - Q^*\right) \\
&+ R_{1m} L^{-1} \varphi + C^{-1} Q - r_c L'^{-1} \varphi \quad \square
\end{aligned} \tag{A.18}$$

References

Anderson, V., Horn, R., & of Mechanical Engineers, A. S. (1967). *American Society of Mechanical Engineers, Tensor Arm Manipulator Design*. American Society of Mechanical Engineers.

Borja, P., Cisneros, R., & Ortega, R. (2016). A constructive procedure for energy shaping of Port-Hamiltonian systems. *Automatica*, *72*, 230–234.

Chikhaoui, M. T., Rabenorosoa, K., & Andreff, N. (2014). Kinematic modeling of an EAP actuated continuum robot for active micro-endoscopy. In J. Lenarčič, & O. Khatib (Eds.), *Advances in Robot Kinematics* (pp. 457–465). Springer International Publishing.

Delgado, S., & Kotyczka, P. (2014). Overcoming the dissipation condition in passivity-based control for a class of mechanical systems. *IFAC Proceedings Volumes*, *47*(3), 11189–11194, 19th IFAC World Congress.

Doria-Cerezo, A., Batlle, C., & Espinosa-Perez, G. (2010). Passivity-based control of a wound-rotor synchronous motor. *IET Control Theory Applications*, *4*(10), 2049–2057.

Duindam, V., Macchelli, A., Stramigioli, S., & Bruyninckx, H. (Eds.), (2009). *Modeling and Control of Complex Physical Systems - The Port-Hamiltonian Approach*. Springer, ISBN 978-3-642-03195-3.

Gutta, S., S.L.ee, J., B.T.rabia, M., & Yim, W. (2009). Modeling of ionic polymer metal composite actuator dynamics using a large deflection beam model. *Smart Materials and Structures*, *18*(11).

Le Gorrec, Y., Zwart, H., & Maschke, B. (2005). Dirac structures and boundary control systems associated with skew-symmetric differential operators. *SIMA Journal on Control and Optimization*, *44*(5), 1864–1892.

Macchelli, A., Le Gorrec, Y., Ramírez, H., & Zwart, H. (2017). On the synthesis of boundary control laws for distributed Port-Hamiltonian systems. *IEEE Transactions on Automatic Control*, *62*(4), 1700–1713.

Maschke, B., & van der Schaft, A. (1992). Port controlled hamiltonian systems: modeling origins and system theoretic properties. In Proceedings of the 3rd IFAC Symposium on Nonlinear Control Systems, NOLCOS'92, Bordeaux, France (pp. 282–288).

Nishida, G., Takagi, K., Maschke, B., & Osada, T. (2011). Multi-scale distributed parameter modeling of ionic polymer-metal composite sofe actuator. *Control Engineering Practice*, *19*(4), 321–334. http://dx.doi.org/10.1016/j.conengprac.2010.10.005.

Ortega, R., & Garcia-Canseco, E. (2004). Interconnection and damping assignment passivity-based control: a survey. *European Journal of Control*, *10*, 432–450.

Ortega, R., van der Schaft, A., Mareels, I., & Maschke, B. (2001). Putting energy back in control. *IEEE Control Systems Magazine*, *21*(2), 18–32.

Ortega, R., van der Schaft, A., Maschke, B., & Escobar, G. (2002). Interconnection and damping assignment: Passivity-based control of port-controlled Hamiltonian systems. *Automatica*, *38*(4), 585–596.

Ramírez, H., Le Gorrec, Y., Macchelli, A., & Zwart, H. (2014). Exponential stabilization of boundary controlled port-hamiltonian systems with dynamic feedback. *IEEE Transactions on Automatic Control*, *59*(10), 2849–2855.

Ramírez, H., Le Gorrec, Y., Maschke, B., & Couenne, F. (2016). On the passivity based control of irreversible processes: A port-Hamiltonian approach. *Automatica*, *64*, 105–111.

Ramírez, H., Maschke, B., & Sbarbaro, D. (2013). Irreversible port-Hamiltonian systems: A general formulation of irreversible processes with application to the CSTR. *Chemical Engineering Science*, *89*, 223–234.

van der Schaft, A. (2017). L_2-Gain and passivity techniques in nonlinear control, *Communications and Control Engineering Series*, (3rd ed.). Springer International Publishing.

van der Schaft, A., & Maschke, B. (2002). Hamiltonian formulation of distributed parameter systems with boundary energy flow. *Journal of Geometry and Physics*, *42*, 166–194.

Shahinpoor, M., & J.K.im, K. (2001). Ionic polymer metal composites: I. fundamentals. *Smart Materials and Structures*, *10*(4), 819.

Webster I.I.I., R. J., & Jones, B. A. (2010). Design and kinematic modeling of constant curvature continuum robots: A review. *International Journal of Robotics Research*, *29*(13), 1661–1683.

Yim, W., Trabia, M. B., Renno, J. M., Lee, J., & Kim, K. J. (2006). Dynamic modeling of segmented ionic polymer metal composite (IPMC) actuator. In 2006 IEEE/RSJ International Conference on Intelligent Robots and Systems (pp. 5459–5464).